Preprints of the 19th World Congress
The International Federation of Automatic Control
Cape Town, South Africa. August 24-29, 2014

Voltage Stability Margins and Risk Assessment in Smart Power Grids

M. Aldeen, S. Saha and T. Alpcan

NICTA, Victoria Research Laboratory,
Department of Electrical and Electronic Engineering, the University of Melbourne, Australia,
(e-mail: aldeen@unimelb.edu.au, sajeebs@unimelb.edu.au, tansu.alpcan@unimelb.edu.au)

Abstract:

This paper presents a quantitative framework for assessment of voltage stability in smart power networks. First, new stability indices similar to gain and phase margins in linear time invariant control systems are introduced. Then, a novel risk assessment framework incorporating the new stability indices is developed to methodologically quantify the voltage stability risks a power system faces at any given operating condition. In contrast to existing local stability indices and qualitative risk approaches, the indices and framework introduced provide analytical and quantitative evaluation of voltage stability and associated risks. The results are illustrated with a numerical example.

Keywords: voltage stability, bifurcation point, voltage collapse, risk, stability indices

1. INTRODUCTION

Power systems are designed to maintain an acceptable voltage profile throughout the network under normal operating conditions as well as after changes in the operating conditions, which could be due to load changes, disturbances, or faults. Voltage instability occurs in power systems when the voltage at a load bus drops well below its nominal value and cannot be brought back by voltage control mechanisms such as reactive power compensators. Abnormal (large) disturbances, unsustainable increase in load demand, or large decrease in power supply may lead to voltage collapse events in power systems. When a power system is heavily stressed (unable to meet the load demand), uncontrollable cascaded events may take place leading to unacceptable levels of voltage drops throughout the network. Therefore, all power distribution grids posses an inherent problem when operating under heavily stressed conditions and are susceptible to voltage instability in absence of adequate compensation schemes. This inherent weakness is likely to feature more prominently in future power grids as the load and generation compositions are expected to undergo a paradigm shift due to the integration of renewable and embedded generation into the grid. Hence the need for a smarter power grids.

To be able to operate power systems in a more intelligent and smarter way, it is essential to be able to ascertain quantitatively the level of stress in the system at any given operating condition. This must be done in terms of metrics that are able to provide a quantitative measure of stability at any given operating condition and the risk of losing it. This requires taking into consideration load characteristics, generators primary control systems such as load-frequency control and reactive power-voltage control, and secondary control mechanism such as StatCom, synchronous condensers, fixed and switched capacitors and tap-changing transformers. Short term (few seconds) voltage instability, for example, occurs shortly after large abnormal events such as faults (Saha & Aldeen, 2011; Saha, Aldeen, & Tan, 2011, 2013). In situations like these, inertial loads and devices which possess reactive power characteristics play a very important role. At the instant immediately after a fault, induction motors draw a large amount of reactive power, and may therefore contribute to the reactive power imbalance in the system and push the system to instability.

Over the past few decades a large amount of literature has appeared dealing with the issue of voltage instability. An early significant result that provides a quantitative measure of voltage stability is reported in (Kessel & Glavitch, July 1986), where an index of voltage stability, that has become to known as the L-index, is introduced. The index, which is a measure of how far the voltage of each node is from reaching the corresponding critical voltage (nose or bifurcation point), can be computed when all node voltages, all generator power angles as well as the network parameters are known or measured on-line. In (Overbye & DeMarco, 1991) the critical point is defined as the saddle node bifurcation (SNB) point rather than traditional nose point. However the analysis is confined to a lossless transmission line. This SNB concept is used in (Jia Hongjie, Yu Xiaodan , & Yixin, 2005) to present an improved stability L_1-index. A test function, based on reduction of the load flow Jacobian to a smaller set of equations is proposed in (Canizares & de Souza, August 1996). The reduction is shown to improve the detection of the static voltage collapse point. This is then followed by (YangWanga, Wenyuan Li, & Lua, 2009) where an equivalent system model and voltage phasors are used to assess an equivalent voltage collapse index. Later (D. Devaraj & J. Preetha Roselyn, 2010) presented an assessment of the voltage stability using ANN. An online voltage stability assessment method using feed forward neural network based on L-index is presented in (S. Kamalasadan , D. Thukaram , & Srivastava, 2009,). In this

method the neural network is trained by using a set of data acquired of the power system (load and generator bus voltages, real and reactive power) under different loading conditions and calculated corresponding L-indices. In (Debbie Q. Zhou, U. D. Annakkage, & Athula D. Rajapakse, 2010) an ANN algorithm is proposed to imitate continuation power flow in order to effectively estimate the nose point of each load bus at any given operating point. The approach uses both bus voltage magnitude and angle obtained from phasor measurement units (PMUs) as the inputs to the ANN along with active/reactive power of both load and generator buses. For optimal placing of PMUs a suboptimal search method is developed in the paper.

The literature on quantitative risk assessment and mitigation is rather limited (Garvey, 2009). One example is the Secure Rank framework (R. A. Miura-Ko & Bambos, 2007) for prioritizing vulnerabilities on a computer network. In the Risk-Rank model of (T. Alpcan & N. Bambos, 2009) risk levels are transferred between components of an organization due to interdependencies between these components. The framework quantitatively keeps track of the risk in an organization by utilizing a diffusion model similar to that of the well-known Page-Rank algorithm used by Google. In(J. Mounzer, T. Alpcan, & N. Bambos, May 2010), an optimization scheme is built on top of this framework, where a system administrator allocates resources to mitigate exposure to risk, and (P. Bommannavar, T. Alpcan, & N. Bambos, June 2011) a game-theoretic extension is developed. The recent work (Y. W. Law, T. Alpcan, M. Palaniswami, & S. Dey, November, 2012) presents a quantitative risk framework for cyber security of smart grid.

In this paper we present a new analytical approach to voltage stability. The approach determines the bifurcation point of any system analytically without having to solve load flow equations or carry out simulation studies as most existing result require. Then we quantify voltage stability in terms of new analytics (metrics). We call these *stability indices*, which are akin to *phase* and *gain margins* used in linear control system theory. The salient advantages of the new approach over existing approaches are: (i) it only uses the *magnitude* of the *bus voltages,* which are already available from the load-flow calculation carried out by power companies to operate their systems, and (ii) it provides exact assessment of indices (no approximation is used). Based on these new stability indices, an analytical framework for voltage stability risk assessment is developed. The framework quantifies voltage stability risks using a probability approach and facilitates explicit cost-benefit analysis and optimisation. Hence, the framework evaluates the stability risk associated with any given system operating point taking into account global characteristics of the system.

The organisation of the paper is as follows. In Section 2, we provide analytical framework to calculate the voltage collapse point. In Section 3, we introduce stability indices to quantify the voltage stability, followed by risk assessment framework in Section 4. In Section 5, we present a numerical example and result analysis. Finally we conclude the paper in section 6.

2. MODEL AND VOLTAGE COLLAPSE POINT

Figure 1 shows a generator bus, *i*, and a load bus, *j*. The complex power balance equation at the generator bus is

$$S_i = P_{Gi} + jQ_{Gi} = S_{Gi} - S_{Di} \tag{1}$$

For the load bus

$$S_{Dj} = S_i + S_k - S_j \tag{2}$$

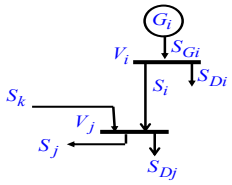

Figure 1: Generator bus connected to a load bus

Consider a simple power system comprising a generator supplying a load at the end of a long transmission line, as shown in Figure 2.

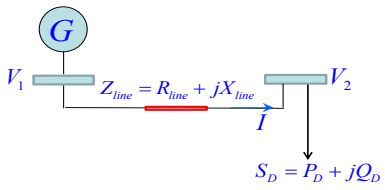

Figure 2: Two Bus Power System

Let the load power factor $pf = \cos\theta_D$ be kept constant. And let

$$\tan\theta_D = \frac{Q_D}{P_D} = \beta \tag{3}$$

The complex power can be expressed as

$$\begin{aligned} S_D = P_D + jQ_D &= V_2 \frac{(V_1 - V_2)^*}{Z_{line}^*} \\ &= Y_{line}^* \left\{ |V_1||V_2| e^{j\delta_{21}} - |V_2|^2 \right\} \end{aligned} \tag{4}$$

where

$$Z_{line} = \frac{1}{Y_{line}}, Y_{line} = G_{line} + jB_{line} = |Y_{line}| \angle\theta_{line} \text{ and } \delta_{21} = \delta_2 - \delta_1$$

or

$$P_D + jQ_D = |Y_{line}||V_1||V_2| e^{j\gamma} - (G_{line} - jB_{line})|V_2|^2 \tag{5}$$

where $\gamma = \delta_{21} - \theta_{line}$.

From equation (5) real and reactive power is expressed as

$$P_D = |Y_{line}||V_1||V_2| \cos\gamma - G_{line}|V_2|^2 \tag{6}$$

or

$$P_D + G_{line}|V_2|^2 = |Y_{line}||V_1||V_2| \cos\gamma \tag{7}$$

and

$$Q_D = |Y_{line}||V_1||V_2| \sin\gamma + B_{line}|V_2|^2 \tag{8}$$

or

$$Q_D - B_{line}|V_2|^2 = |Y_{line}||V_1||V_2| \sin\gamma \tag{9}$$

After squaring both sides of equation (7) we obtain

$$P_D^2 + 2P_D G_{line}|V_2|^2 + G_{line}^2|V_2|^4 = \{|Y_{line}||V_1||V_2|\}^2 \cos^2\gamma \quad (10)$$

Similarly from equation (9) we obtain

$$Q_D^2 - 2Q_D B_{line}|V_2|^2 + B_{line}^2|V_2|^4 = \{|Y_{line}||V_1||V_2|\}^2 \sin^2\gamma \quad (11)$$

Using equation (3) in (11) we write

$$\beta^2 P_D^2 - 2\beta P_D B_{line}|V_2|^2 + B_{line}^2|V_2|^4 = \{|Y_{line}||V_1||V_2|\}^2 \sin^2\gamma \quad (12)$$

Addition of equations (10) and (12) gives

$$|V_2|^4|Y_{line}|^2 + |V_2|^2\{2P_D(G_{line} - \beta B_{line}) - |Y_{line}|^2|V_1|^2\} + P_D^2(1+\beta^2) = 0 \quad (13)$$

The solution to equation (13) is

$$|V_2|^2 = \frac{|Y_{line}|^2|V_1|^2 - 2P_D(G_{line} - \beta B_{line})}{2|Y_{line}|^2} \pm \frac{\sqrt{\{2P_D(G_{line} - \beta B_{line}) - |Y_{line}|^2|V_1|^2\}^2 - 4|Y_{line}|^2 P_D^2(1+\beta^2)}}{2|Y_{line}|^2} \quad (14)$$

This is an exact solution of load bus voltage at any given operating condition and load power factor.

2.1 Calculation of Critical (Bifurcation) Point

Critical voltage also called nose or bifurcation point is a condition where the bus voltage is about to transit from the stable to unstable region and thus no amount of load shedding can restore it back to stability. At this point the amount of power that can be drawn by the load at the bus is maximum, beyond which the system become voltage unstable. From equation (14), it is clear that maximum load power that causes voltage collapse occurs when the term in the square root is zero, i.e. when the following condition is satisfied

$$\{2P_{D_{cr}}(G_{line} - \beta B_{line}) - |Y_{line}|^2|V_1|^2\}^2 - 4|Y_{line}|^2 P_{D_{cr}}^2(1+\beta) = 0 \quad (15)$$

Once maximum power is computed from the solution of equation (15), the critical voltage for each bus can be computed from

$$|V_{2_{cr}}|^2 = \frac{|Y_{line}|^2|V_1|^2 - 2P_{D_{cr}}(G_{line} - \beta B_{line})}{2|Y_{line}|^2} \quad (16)$$

Equations (15) and (16) provide an exact identification of the bifurcation (critical) point.

3. STABILITY INDICES

Voltage stability is a measure of how far an operating point is from the critical point. Three new indices are introduced in this paper to quantify voltage stability. They are: (i) phase margin, (ii) gain margin, or (iii) incremental area under the P-V curve, as illustrated in Figure 3. These measures can be assessed on line every time a load flow is carried out, as explained in detail below.

3.1 Phase Margin (PM)

In control system theory, phase margin is widely used to ascertain system stability, analogous to which we define phase margin (PM) as a measure of voltage stability of a power system. It may be seen from the P-V curve (Figure 3) that at voltage collapse point, slope of the P-V curve is

$$\phi_{cr} = \tan^{-1}\left.\frac{\partial V_2}{\partial P_D}\right|_{cr} = 90^\circ \quad (17)$$

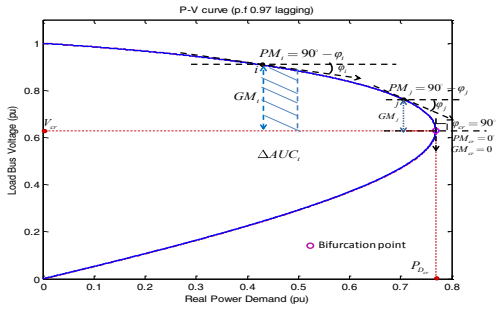

Figure 3: PV curve showing proposed stability indices

where the system becomes unstable. Phase margin at an operating point i is the measure of angular difference between the angle ϕ_i measured at point i (obtained from the slope P-V curve at that operating point) and the angle of P-V curve at the voltage collapse point, which is $\phi_{cr} = 90^\circ$. Mathematically PM is expressed as

$$\text{PM}_i = 90^\circ - \phi_i \quad (18)$$

where $\phi_i = \tan^{-1}\left.\frac{\partial V_2}{\partial P_D}\right|_i$ is the P-V curve slope at the operating point i. From Figure 3, it may be seen that as the load demand increases, the slope of the P-V curve also increases. Hence, from equation (18) it is obvious that phase margin decreases as the load demand increases. As the load demand reaches the critical loading value i.e. P_{Dcr} the phase margin becomes zero. This is illustrated in Figure 3.

$\left.\frac{\partial V_2}{\partial P_D}\right|_i$ may be calculated from the Jacobian matrix (J) at any operating point, which is a result of the load-flow calculations , where the Jacobian at operating point i is defined as

$$J_i = \begin{bmatrix} \left.\frac{\partial P_2}{\partial V_2}\right|_i & \left.\frac{\partial P_2}{\partial \delta_2}\right|_i \\ \left.\frac{\partial Q_2}{\partial V_2}\right|_i & \left.\frac{\partial Q_2}{\partial \delta_2}\right|_i \end{bmatrix} \quad (19)$$

3.2 Gain Margin (GM)

As described in section 2, at the critical voltage or bifurcation point, the bus voltage (V_{cr}) transits from the stable to

unstable region and no amount of load shedding can restore it back to stability. In analogy to gain margin (measure of stability) used in linear control system theory, we introduced a stability index called gain margin (*GM*). The gain margin is defined as the distance of an operating point from the critical point. This can be quantified by measuring the load bus voltage at operating point i (V_{2i}) and subtract it from the critical voltage, V_{2cr}, computed from equation (16), i.e.

$$GM_i = V_{2cr} - V_{2i} \tag{20}$$

From Figure 3, it may be seen that as the load demand increases, the load bus voltage decreases. Hence from equation (20), it is obvious that gain margin decreases as load power demand increases. Eventually, as the load demand reaches the critical loading condition P_{Dcr} the gain margin becomes zero. Therefore, as in control systems, the proximity of GM to zero is an indication of how close the system is to voltage instability.

3.3 Incremental Area Under the Curve (ΔAUC)

Another stability measure introduced in this paper is incremental area under the curve (ΔAUC). It may be seen from Figure 3 that, for lagging power factor loads, as the load demand increases the incremental area under the P-V curve decreases and eventually becomes zero, once the power demand reaches the critical value P_{Dcr}. This stability measure can be computed at any given operating point as follows

$$\Delta AUC_i = \int_{P_{Di}}^{P_{Di}+\Delta} V_2(P_D)\,dP_D - \Delta * V_{cr} \tag{21}$$

Remark 1: It may be worth noting that proposed stability indices describe three different aspect of system stability. The phase margin (PM) stability index describes how fast the system is heading towards the voltage collapse point; gain margin (GM) describes how far the system is from the voltage collapse point and the incremental area under the curve (ΔAUC) stability index describes incremental change in net energy in the system as the power demand increases towards the critical value P_{Dcr}.

3.4 Standardisation of Indices

In order to have a standard measure of voltage stability, the above three indices are presented in terms of per unit values. For lagging power factor load case, let $S(P_0)$ (stability index at no load) denote the base value of any of the three stability indices and $S(P_{Di})$ is the value at any operating condition i. Then the per unit value of the index is computed as

$$S_{pu} = \frac{S(P_{Di})}{S(P_0)} \tag{22}$$

In the case of leading power factor loads, the load acts as a reactive power source and injects reactive power at the bus. The amount of reactive power injection increases as the load demand increases thus providing voltage support at the load bus. However a point will be reached when the amount of reactive power used by the line is equal to the reactive power injected by the load. At this load demand $\left(P_{D,V_2\max}\right)$, load bus voltage is maximum $\left(V_{2\max}\right)$. From then on the system behaves the same as that of lagging power factor i.e. the reactive power requirement of the lines is larger than that provide by the load and generator. This deficit will continue to increase with the increase in the load demand until the critical point is reached. In order to conform to the lagging power factor case, we define $S(P_{D,V_2\max})$ as the base for the leading power factor load. So for leading power factor loads, the per unit value of the index is computed as

$$S_{pu} = \frac{S(P_{Di})}{S(P_{D\max})} \tag{23}$$

3.5 Calculation of $P_{D,V_2\max}$

From equation (13) we have

$$|V_2|^4|Y_{line}|^2 + |V_2|^2\left\{2P_D(G_{line}-\beta B_{line}) - |Y_{line}|^2|V_1|^2\right\} + P_D^2(1+\beta^2) = 0 \tag{24}$$

Differentiating equation (24) with respect to P_D we obtain

$$\frac{\partial|V_2|}{\partial P_D} = \frac{-|V_2|^2\,2(G_{line}-\beta B_{line}) - 2P_D(1+\beta^2)}{\left[4|V_2|^3|Y_{line}|^2 + 2|V_2|\left\{2P_D(G_{line}-\beta B_{line}) - |Y_{line}|^2|V_1|^2\right\}\right]} \tag{25}$$

Setting equation (25) to zero, we find the maximum voltage in terms of $P_{D,V_2\max}$ as

$$-|V_2|^2_{\max}\,2(G_{line}-\beta B_{line}) - 2P_{D,V_2\max}(1+\beta^2) = 0 \tag{26}$$

or

$$|V_2|^2_{\max} = -\frac{(1+\beta^2)}{(G_{line}-\beta B_{line})}P_{D,V_2\max} = \psi P_{D,V_2\max} \tag{27}$$

Substituting (27) into (13) obtain the following loading condition for which the voltage reaches its maximum value

$$P_{D,V_2\max} = \frac{\psi Y_{line}^2|V_2|^2_{\max}}{\psi Y_{line}^2 - \left(1+\beta^2\right)} \tag{28}$$

Equations (27) and (28) provide the operating condition where the load voltage reaches maximum value for leading (capacitive) loads. For such loads, we can identify three regions of operations: (i) To the left of $P_{D,V_2\max}$ point the system has surplus reactive power which provides voltage support, (ii) at this point the surplus become zero, which means that the surplus reactive power is now used by the line due to the increase in the load and thus line current, and (iii)

to the right of this point the system has deficit reactive power, which means that the system in this region starts to loss its ability to provide reactive power support for the line culminating in total collapse at the critical loading condition.

4. RISK ASSESSMENT FRAMEWORK

The voltage stability indices introduced in the previous sections provide a solid foundation for quantitative assessment of voltage stability risks. While these indices are useful for evaluating system voltage stability at any given operating point, a comprehensive methodology is necessary for assessing and mitigating voltage stability risks. In this respect we next introduce an analytical framework for voltage stability risk assessment. The framework quantifies voltage stability risks by using a probability approach and facilitates explicit cost-benefit analysis and optimisation as depicted in Figure 4. Hence, the framework provides a vehicle for making informed decisions on assessing and mitigating risks.

There are multiple definitions of risk and the word is "overloaded" due to its common usage in daily life. The definition of risk adopted in this paper is a probabilistic one and can be summarised as "the probability of a bad event happening times the magnitude of the bad event" (Hubbard, 2009). To formalise this definition, let E be the universal set which contains the voltage collapse event, e, corresponding to the system reaching the critical point and the default event of the system staying away from the critical point denoted by n. Then, we define the set E as $E = \{e, n\}$.

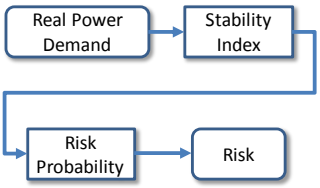

Figure 4: Risk Assessment Framework

The probability of the event, e, of the system reaching a critical point is defined as $P(e)$. In general, the risk probability is expressed as $P_{voltage} = max_{e \in E} P(e)$. The magnitude of the voltage collapse event, e, e.g. the monetary damage a (partial) voltage collapse would cause, is captured by the function $M(e)$. Here, the voltage instability will result in a damage quantified by the amount M which follows from the cost of the load shedding when the system reaches the critical point. Thus, the voltage stability risk $R_{voltage}$ is formally defined as

$$R_{voltage} := P_{voltage} \times M \tag{29}$$

The impact of a voltage collapse event, M, is more related to the business aspects of the problem. It can be quantified based on the characteristics of the specific power system which determines its scope, legal requirements, and the service level agreements with customers. In this paper we define M as

$$M(\$/MWh) = P_{Dcr} \times VCR \tag{30}$$

where P_{Dcr} is the real power demand at the critical or bifurcation point and the "value of customer reliability or $VCR(\$/kWh)$ (AEMO, 2012)" is used to describe the 'value of lost load' or 'customer cost of service interruption, or simply 'outage cost'. The VCR used in this paper is the official one published by the Australian Energy Market Operator (AEMO) in 2012 with the purpose of estimating the marginal value of reliability to electricity consumers. It is a composite value of all sectors (residential, commercial, agricultural, and industrial), which is based on surveys designed to estimate the costs faced by consumers as a result of electricity supply interruptions.

The calculation of the risk probability $P_{voltage}$, however, is a function of the system operating point. The stability indices developed in the previous sections are hence essential for a methodological assessment of the risk probability.

There is clearly more than one way of devising a risk probability measure. We have, therefore, chosen an axiomatic approach in this paper. The axioms are based on the voltage stability indices introduced in the section 3. In this paper, we introduce the following three axioms which together define a class of risk probability functions.

A1. *$P_{voltage}$ is a probability measure, i.e.* $0 \le P_{voltage} \le 1$.

A2. *$P_{voltage}$ =1 at critical point, and* $P_{voltage} \ge 0$ *at other stable operating points.*

A3. *$P_{voltage}$ is non-decreasing in the "distance" between the system operating point and the closest critical point as quantified by a stability index.*

A variety of functions mapping the stability index to risk probability can satisfy the axioms *A1-A3*. Among others, we propose two such functions that relate to the either of the three stability indices; a linear function defined as

$$P_{voltage}(P_{Di}) = 1 - S_{pu}(P_{Di}) \tag{31}$$

where S_{pu} is the per unit index defined in equations (22) for lagging power factor loads or (23) for leading power factor loads. This index could be any of the three indices introduced in the section 3 (phase margin, gain margin or incremental area under the curve) at a given operating point P_{Di}. An alternative family of functions satisfying the Axioms *A1-A3* is

$$P_{voltage}(P_{Di}) = 1 - e^{-\alpha\left(\frac{S_{\max} - S_{pu}(P_{Di})}{S_{pu}(P_{Di})}\right)} \tag{32}$$

where $S_{max} = \max\left(S_{pu}(P_{Di})\right), \forall i$ (operating point) and α is a calibration parameter. For $\alpha > 1$ the mapping represents a "*risk averse*" approach and for $\alpha < 1$ the mapping captures a "*risk taking*" approach. In order to attain a consistent risk probability measure across all three stability indices, we determine the calibration parameter α from the slope of the (

$\frac{\partial P_{Di}}{\partial V_i} - V_i$) curve. Thus, the risk (probability) maps the system operating point to a real value within the range [0,1] quantifying the risk state of the system at any given operating point.

5. APPLICATION EXAMPLE AND ANAYSIS OF RESULTS

Two bus power system shown in Figure 2 is considered as the example power system in this paper, where a single machine is connected to a load through a transmission line $(Z_{line} = 0.01 + j0.5 pu)$. Family of P-V curves and corresponding bifurcation points for different power factor loads are shown in Figure 5. First we will analyse the results for lagging power factor and unity power factor load.

5.1 Lagging and unity power factor load case

Under no load conditions, since there is no power transfer from source bus to the load bus, the voltage (both magnitude and angle) at both buses are the same, i.e. $V_1 = V_2 = 1\angle 0^\circ \; pu$. In order to meet the increase in power demand at the load bus, the source (generator bus, i.e. bus 1 in the example system) needs to transfer power equal to the sum of load demand and the loss in the transmission line (both real $(I^2 R_{line})$ and reactive $(I^2 X_{line})$).

Active power transfer from generator to load may be approximated by

$$P_G = \frac{|V_1||V_2|}{X_{line}} \sin\delta \tag{33}$$

where $\delta = (\delta_1 - \delta_2)$ is called the power angle. To meet the increase in the load demand, with V_2 decreasing, the power angle must increase, as V_1, X_{line} are fixed. On the other hand, reactive power transfer from the source to the load is approximated by

$$Q_G \cong \frac{|V_1|(|V_1| - |V_2|\cos\delta)}{X_{line}} \tag{34}$$

Thus an increase in δ accompanied by a decrease in V_2 will result in an increase in the amount of reactive power supplied by the generator. The amount of reactive power used in the transmission line is approximated as

$$Q_{line} \cong \frac{(V_1 - V_2)^2}{X_{line}} \tag{35}$$

It is therefore clear that incremental reactive power used in the line is higher than that supplied by the generator, i.e.

$$\Delta Q_{line} > \Delta Q_G = \frac{|V_1|(|V_1| - |\Delta V_2|\cos\Delta\delta)}{X_{line}} \tag{36}$$

Thus it can be concluded from equation (36) that the reactive power deficit in the system will increase as the load demand increase. This deficit will grow to the point where the generator's capacity is fully utilised and no additional reactive power injection is possible. This point is the critical (bifurcation) point.

Figure 5 shows that, for loads with higher power factor the effect of load increases on the voltage level is less severe. For example, loads with unity power factor are more tolerant to load increases than loads with to 0.98 lagging because of the availability of extra reactive power. This illustrated by the different bifurcation points in Figure 5 where high power factor loads have their critical points occurring to higher load and voltage levels. The above analysis is also clearly demonstrated in (Figure 6(a) - Figure 8(a)), where proposed stability margins $(PM, GM, \Delta\text{AUC})$ are shown to decrease at different rates (the highest is caused by the lowest power factor) as the load demand increases. At the bifurcation point, the stability margins become zero, which means that system is about to transit from the stable to unstable regions. Once this point is breached, no amount of load shedding or reactive power compensation can restore the voltage to normality. On the contrary, load shedding after reaching bifurcation point, will only exacerbate the voltage decline as shown in Figure 5.

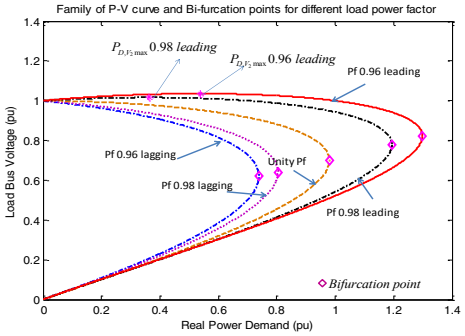

Figure 5: Family of P-V curve for the Example power system load bus

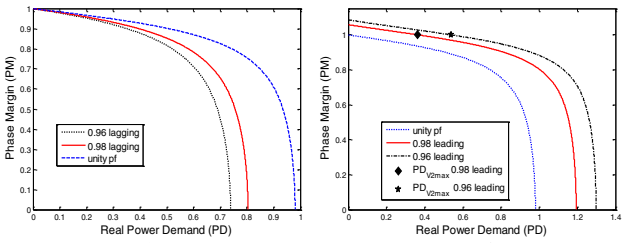

(a) (b)

Figure 6: Phase Margin

Figure 9 (a) - Figure 11 (a) shows the risk probability calculated using proposed stability margins PM, GM and ΔAUC respectively. It may be seen from the figures that the risk probability increases slowly initially with the increases in real power demand. But as the load demand increases closer to the critical value P_{Dcr} the risk probabilities surges to unity stating that the system has reached the critical point.

5.2 Leading power factor load case

In the case of leading power factor loads, the load injects reactive into the system. However, real power is still supplied by the generator to the rest of the system. As the load demand increases, then it is clear that from equation (33) that the power angle δ increases. The increase in the load demand is

accompanied by an increase in the reactive power injection into the system by the load itself. If this increase is larger than the reactive power used by the line, the load bus voltage increases. From equation, it is obvious that with the increase in the load angle δ the load bus voltage increase as shown by the P-V curves in Figure 5 for the two leading power factor loads i.e. 0.98 and 0.96 leading.

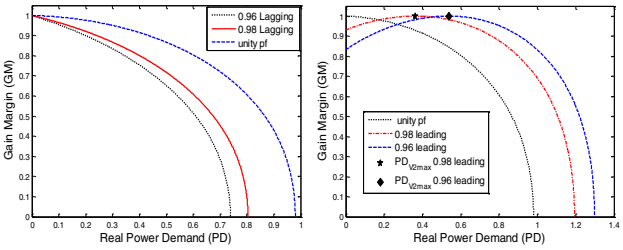

(a) (b)

Figure 7: Gain Margin

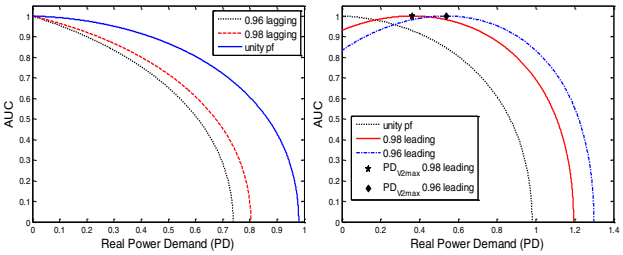

(a) (b)

Figure 8: Area under the Curve

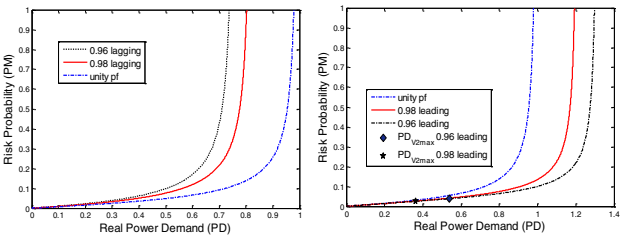

(a) (b)

Figure 9: Risk Probability (Calculated using stability index PM)

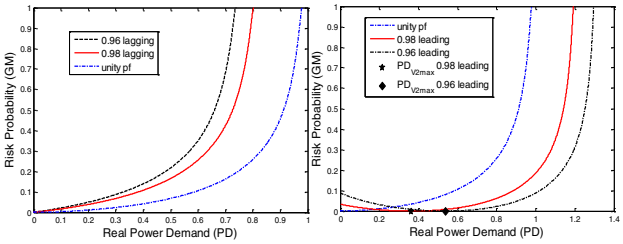

(a) (b)

Figure 10: Risk Probability (Calculated using stability index GM)

As the load demand further increases, the reactive power used by the line increases until becomes equal to that supplied by the load bus. At this load demand ($P_{D,V_2\max}$) the load bus voltage is maximum ($V_{2\max}$) as shown in Figure 5. Beyond $P_{D,V_2\max}$ load demand, the system behaves exactly the same as that of a lagging power load. Eventually, the critical or bifurcation point is reached (as shown by the diamond symbol in Figure 5) when the reactive power used in the line cannot be satisfied.

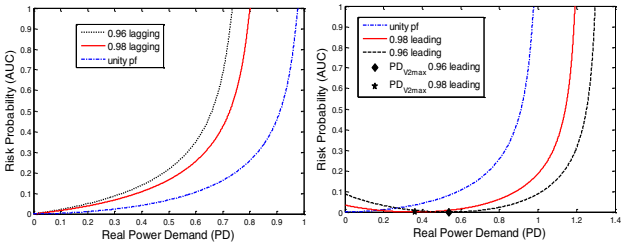

(a) (b)

Figure 11: Risk Probability (Calculated using stability index AUC)

Phase margin for leading power factor case is shown in Figure 6(b). As explained above, the increase in load demand up to $P_{D,V_2\max}$ brings about an increase in the load bus voltage (from P-V curve Figure 5). However the rate of increase in the load bus voltage, as shown in the P-V curve, decreases from maximum (PM> 90°) at no lead to zero (PM= 90°) at $P_{D,V_2\max}$. Using $PM(P_{D,V_2\max})$ as the base value, it follows that phase margin (in per unit) is higher than unity ($PM>1$) at the no load condition and is unity ($PM=1$) at $P_{D,V_2\max}$. Once load power demand increases to more than $P_{D,V_2\max}$, the phase margin decreases and becomes 0 at P_{Dcr}.

Remark 2: It may be worth noting that for leading power factor load, phase margin stability index may be sub divided in two regions

i) $PM \geq 1$ (for $0 \leq P_D \leq P_{D,V_2\max}$). In this region, the system stability enhances as load demand increases. But the stability enhancement rate decreases with the increment of load demand (as the voltage increment rate decreases) and becomes zero (as the voltage increment rate is zero) at $PM=1$ $\left(P_D = P_{D,V_2\max}\right)$.

ii) $0 \leq PM \leq 1$ (for $P_{D,V_2\max} \leq P_D \leq P_{Dcr}$). In this region the system behaves similarly as that with a lagging power factor load.

Gain margin for leading power factor load is shown in Figure 7(b). The increase in load demand up to $P_{D,V_2\max}$ brings about an increase in the gain margin, as the load bus voltage increases. The *GM* attains maximum value when the load demand reaches $P_{D,V_2\max}$, as at this point the load bus voltage increases to a maximum value. This indicates that system is most stable at load demand $P_{D,V_2\max}$. Once the load power demand increases to more than $P_{D,V_2\max}$, the gain margin decreases and becomes 0 at P_{Dcr}. Stability index ΔAUC is shown in Figure 8(b) which may be analysed similarly as the stability index *GM*.

Risk probability calculated using *PM* is shown in Figure 9 (b). As the *PM* decreases with the increase in load demand, the risk probability increases exponentially and becomes 1 (maximum) at load demand P_{Dcr}. If *GM* and ΔAUC are associated with risk probability, form Figure 10(b) and Figure 11 (b) we can see that risk probability decreases to zero at load demand $P_{D,V_2\max}$. This states that system is most

stable at load demand $P_{D,V_2\max}$. Beyond this point ($P_{D,V_2\max}$), the system behaves exactly the same as the lagging power factor load case, i.e. as the load demand increases the risk probability increases.

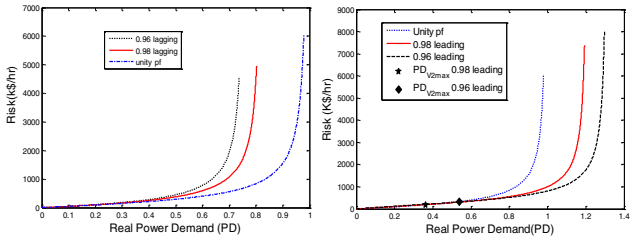

(a) (b)

Figure 12: Risk (Calculated using stability index PM)

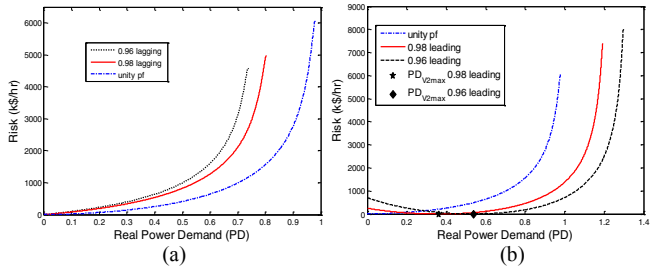

(a) (b)

Figure 13: Risk (Calculated using stability index GM)

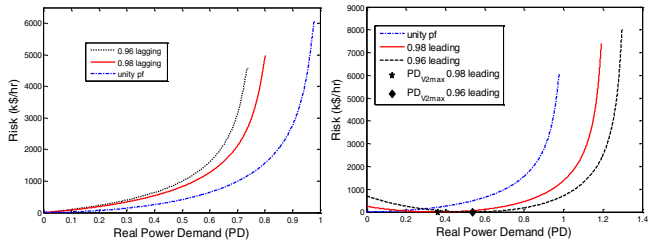

(a) (b)

Figure 14: Risk (Calculated using stability index AUC)

Figure 12 - Figure 14 shows risk (in terms of financial loss (dollar values)) associated with the increment of load demand in the example power system. When the load demand increases to critical value P_{Dcr}, the system becomes unstable and P_{Dcr} amount of load is lost. Financial loss (due to the loss of power demand P_{Dcr}) is associated with value of lost load, $VCR(\$/kwh)$, as shown in equation (30). In this paper, the VCR value, $\$61.83/kWh$, published by the Australian Energy Market operator (AEMO) for the Victoria State of Australia is used and the system base is considered to be 100 MVA. It may be seen from Figure 12 - Figure 14 that financial risk increases as load demand increases and approaches maximum value at the critical value of load demand, P_{Dcr}.

6. CONCLUSION

New quantitative metrics for on-line assessment of voltage stability in power networks and associated risk analysis is presented in this paper. First, new stability indices similar to gain and phase margins in linear time invariant control systems are introduced. Then, a novel risk assessment framework incorporating the new stability indices is developed to methodologically quantify the voltage stability risks a power system faces at any given operating condition. In contrast to existing local stability indices and qualitative risk approaches, the proposed indices and framework provide a global and quantitative evaluation of voltage stability and associated risks. The results are illustrated with a numerical example. The extension to generic scalable multi-machine case is under investigation.

7. ACKNOWLEDGEMENT

This research is supported by National ICT Australia and the Austrian Research Council through the Discovery Grant (ARC-DP140102180).

8. REFERENCES

AEMO. (2012). *National Value for customer reliability (VCR)* (No. 2).

Canizares, C. A., & de Souza, A. C. Z. (August 1996). Comparison of Performance Indices for Detection of Proximity to Voltage Collapse. *IEEE Transactions on Power Systems, 11*(3), 1441-1450.

D. Devaraj , & J. Preetha Roselyn. (2010). Genetic algorithm based reactive power dispatch for voltage stability improvement. *Electrical Power and Energy Systems, 32*, 1151-1156.

Debbie Q. Zhou, U. D. Annakkage, & Athula D. Rajapakse. (2010). Online Monitoring of Voltage Stability Margin Using an Artificial Neural Network. *IEEE Trans. on PAS, 25*(3), 1566-1574.

Garvey, P. R. (2009). *Analytical Methods for Risk Management: A Systems Engineering Perspective*. Boca Raton, FL, USA: Chapman and Hall/CRC.

Hubbard, D. W. (2009). *The Failure of Risk Management: Why It's Broken and How to Fix It*: Wiley.

J. Mounzer, T. Alpcan, & N. Bambos. (May 2010). *Dynamic control and mitigation of interdependent IT security risks*. Paper presented at the IEEE Conference on Communication (ICC).

Jia Hongjie, Yu Xiaodan , & Yixin, Y. (2005). An improved voltage stability index and its application. *Electrical Power and Energy Systems, 27*, 567-574.

Kessel, P., & Glavitch, H. (July 1986). Estimating the voltage stability of power systems. *IEEE Transactions on Power Delivery, 1*, 346-354.

Overbye, T. J., & DeMarco, C. L. (1991). Improved techniques for power system voltage stability assessment using energy methods. *IEEE Trans. on PAS, 6*(4), 1446-1452.

P. Bommannavar, T. Alpcan, & N. Bambos. (June 2011). *Security risk management via dynamic games with learning*. Paper presented at the IEEE Intl. Conference on Communications (ICC).

R. A. Miura-Ko, & Bambos, N. (2007). *Securerank: A risk-based vulnerability management scheme for computing infrastructures*. Paper presented at the IEEE Conference on Communication ICC. IEEE.

S. Kamalasadan , D. Thukaram , & Srivastava, A. K. (2009,). A new intelligent algorithm for online voltage stability assessment and monitoring. *International Journal of Electrical Power & Energy Systems, 31*(2-3), 100-110.

Saha, S., & Aldeen, M. (2011). *Modelling of transmission line faults in power system*. Paper presented at the 31st IASTED international conference on modelling, identification and control.

Saha, S., Aldeen, M., & Tan, C. P. (2011). Fault detection in transmission networks of power systems. *International Journal of Electrical Power & Energy Systems, 33*(4), 887-900.

Saha, S., Aldeen, M., & Tan, C. P. (2013). Unsymmetrical Fault Diagnosis in Transmission/Distribution Networks *International Journal of Electric Power and Energy Systems, 45*(1), 252-263.

T. Alpcan, & N. Bambos. (2009). *Modeling dependencies in security risk management*. Paper presented at the CRiSIS. IEEE.

Y. W. Law, T. Alpcan, M. Palaniswami, & S. Dey. (November, 2012). *Security Games and Risk Minimization for Automatic Generation Control in Smart Grid*. Paper presented at the 3rd Conference on Decision and Game Theory for Security (GameSec).

YangWanga, Wenyuan Li, & Lua, J. (2009). A new node voltage stability index based on local voltage phasors. *Electric Power Systems Research 79*, 265-271.